Imaging Science in Dentistry 2024; 54: 147-57
https://doi.org/10.5624/isd.20230249

Correlation between cone-beam computed tomographic findings and the apnea-hypopnea index in obstructive sleep apnea patients: A cross-sectional study

Marco Isaac[1,2], Dina Mohamed ElBeshlawy[2,3], Ahmed Elsobki[4], Dina Fahim Ahmed[2], Sarah Mohammed Kenawy[2,*]

[1]*Department of Oral and Maxillofacial Radiology, Faculty of Oral and Dental Medicine, Delta University for Science and Technology, Gamasa, Egypt*
[2]*Department of Oral and Maxillofacial Radiology, Faculty of Dentistry, Cairo University, Cairo, Egypt*
[3]*Department of Oral and Maxillofacial Radiology, Galala University, Sokhna, Egypt*
[4]*Department of Oral and Maxillofacial Radiology, Mansoura University, Mansoura, Egypt*

ABSTRACT

Purpose: The aim of this study was to explore the correlations of cone-beam computed tomographic findings with the apnea-hypopnea index in patients with obstructive sleep apnea.
Materials and Methods: Forty patients with obstructive sleep apnea were selected from the ear-nose-throat (ENT) outpatient clinic, Faculty of Medicine, Mansoura University. Cone-beam computed tomography was performed for each patient at the end of both inspiration and expiration. Polysomnography was carried out, and the apnea-hypopnea index was obtained. Linear measurements, including cross-sectional area and the SNA and SNB angles, were obtained. Four oral and maxillofacial radiologists categorized pharyngeal and retropalatal airway morphology and calculated the airway length and volume. Continuous data were tested for normality using the Kolmogorov-Smirnov test and reported as the mean and standard deviation or as the median and range. Categorical data were presented as numbers and percentages, and the significance level was set at $P<0.05$.
Results: The minimal value of the cross-sectional area, SNB angle, and airway morphology at the end of inspiration demonstrated a statistically significant association ($P<0.05$) with the apnea-hypopnea index, with excellent agreement. No statistically significant difference was found in the airway volume, other linear measurements, or retropalatal airway morphology.
Conclusion: Cone-beam computed tomographic measurements in obstructive sleep apnea patients may be used as a supplement to a novel radiographic classification corresponding to the established clinical apnea-hypopnea index classification. ***(Imaging Sci Dent 2024; 54: 147-57)***

KEY WORDS: Sleep Apnea, Obstructive; Cone-Beam Computed Tomography; Airway Obstruction

Introduction

Sleep breathing disorders have a negative impact on the public quality of life. These disorders encompass a wide range of abnormalities in respiratory function, including hypoxia, sleep fragmentation, and obstructive sleep apnea (OSA). Approximately 936 million people around the world have been diagnosed with OSA, making it the most common sleep-breathing disorder.[1] This condition, which affects 14% of men and 5% of women, is characterized by an obstruction of airflow in the upper airway accompanied by a respiratory effort that can cause frequent, unexpected awakenings during the night, as well as oxygen desaturation.[2]

Polysomnography is the gold-standard diagnostic procedure for OSA. Polysomnography uses electroencephalography, electrooculography, electrocardiography, pulse oximetry, and airflow and respiratory effort measurements to calculate the apnea-hypopnea index (AHI), which mea-

Received November 16, 2023; Revised January 22, 2024; Accepted January 29, 2024
Published online April 2, 2024
*Correspondence to : Prof. Sarah Mohammed Kenawy
Department of Oral and Maxillofacial Radiology, Faculty of Dentistry, Cairo University, 11 El-Saraya Street, Manial, Cairo, Egypt
Tel) 20-2-23634965, E-mail) sarah.kenawy@dentistry.cu.edu.eg

Imaging Science in Dentistry · pISSN 2233-7822 eISSN 2233-7830

sures the number of times an individual's airflow was obstructed during 1 hour of sleep.[3,4] To be diagnosed with OSA, a patient must have an AHI of 15 or more events per hour, or 5 or more events per hour if symptoms or cardiovascular comorbidities are present.[5] OSA is classified as mild (AHI = 5-15 events/hour), moderate (AHI = 15-30 events/hour), or severe (AHI = 30 events/hour) based on the AHI cutoff references and thresholds.[1,6,7] Many factors are assessed during a polysomnography exam, but the most crucial ones are oxygen saturation and the AHI, both of which are primarily used to confirm an OSA diagnosis. Polysomnography is a high-cost procedure, both monetarily and in terms of personnel, facilities, and specialized consultants.[8] Additionally, because of the restricted availability of polysomnography and the constraints associated with its accessibility, there are currently very long waiting lists, which exacerbate the illness burden.[9] Nonetheless, current knowledge and recognition of OSA in primary care are crucial to managing the disease process.[10-12] OSA specialists, dentists trained in sleep medicine, and physical therapists must collaborate closely to create the most effective pathway from diagnosis to treatment.[13]

Cone-beam computed tomography (CBCT) imaging produces 3-dimensional (3D) images and provides an extremely accurate assessment of craniofacial and upper airway anatomy. CBCT offers less X-ray exposure than traditional computed tomography (CT) and good-quality radiographic images. While CBCT cannot diagnose OSA, it is an essential tool for evaluating various anatomical features, such as volume, surface area, cross-sectional area, angles, and shapes. These features are critical for physicians to determine the origin, severity, and prognosis of the disorder, as CBCT is a valuable imaging technique for delineating the boundaries of soft tissues.[14] To sum up, advancements in CBCT technology have opened up numerous opportunities for upper airway evaluation.[15,16]

In this context, the present study investigated the correlations of CBCT findings, including pharyngeal and retropalatal airway morphology and linear and volumetric measurements, with the AHI in patients with OSA.

Materials and Methods

All patients were recruited from the outpatient clinics of the ear-nose-throat (ENT) department of Mansoura University, Faculty of Medicine, Egypt. Eligible patients were adults over the age of 18 who were candidates for upper respiratory airway surgery, as determined by a comprehensive history, clinical examination, and polysomnography. Each patient was informed about the purpose of the study and provided with all relevant information before giving their written consent to participate. The Faculty of Dentistry, Cairo University, Research Ethical Committee granted approval in line with the Helsinki Declaration of 1964. To maintain participant confidentiality and to ensure the integrity of the blinding procedure, all reports, personal data, scans, and administrative documents were securely stored and identified only by a unique coded identification (ID) number. The study was registered at www.clinicaltrials.gov with the ID: OCS05051989 on January 26, 2021.

The sample size calculation was based on a study that investigated correlations between the upper airway length on cephalometric images and the severity of OSA.[17] The calculation utilized a correlation coefficient and was conducted with the following formula, the standard normal deviation for $\alpha = Z\alpha = 1.9600$, the standard normal deviation for $\beta = Z\beta = 1.2816$, $C = 0.5 \times \ln[(1+r)/(1-r)] = 0.5763$, and the total sample size $= N = [(Z\alpha + Z\beta)/C]2 + 3 = 35$. After adding 10% to compensate for dropout, the total sample size was 40 OSA patients.

An ENT multidisciplinary team was assigned to assess and determine which OSA patients to enroll based on whether they would benefit from this study. At first, a thorough study of each patient's background was carried out, including a review of all potential risk factors and a full account of the patient's sleep behaviors.[18] Next, the oropharynx, nasopharynx, and hypopharynx were clinically examined in detail for signs of pathology or structural anomalies, such as nasal airway obstruction, an overly long soft palate or uvula, and swollen lingual tonsils. Patients filled out the Epworth Sleepiness Scale (ESS), an 8-part questionnaire that measures how often a person nods off during everyday activities.[19,20] Then, polysomnography was performed to properly evaluate normal and pathological physiological sleep episodes. Body mass index (BMI) was recorded, and the AHI was used to determine the severity of OSA, and patients were categorized as mild, moderate, and severe.[21]

Using the iCAT FLX V17-Series CBCT system (Imaging Science International, ISI, Hatfield, PA, USA), 2 radiographic examinations–at the end of inspiration and end of expiration–were performed before surgical intervention. Quick scan imaging methodology using a field of view (FOV) of 16 cm × 13 cm (120 kVp, 5 mA, 2 s) with a voxel size of 0.3 mm was applied. During scanning, participants wore a protective lead apron. Participants were instructed to remain stable, hold their breath for only 2 s, and not move their head, body, tongue, or jaws. Sub-

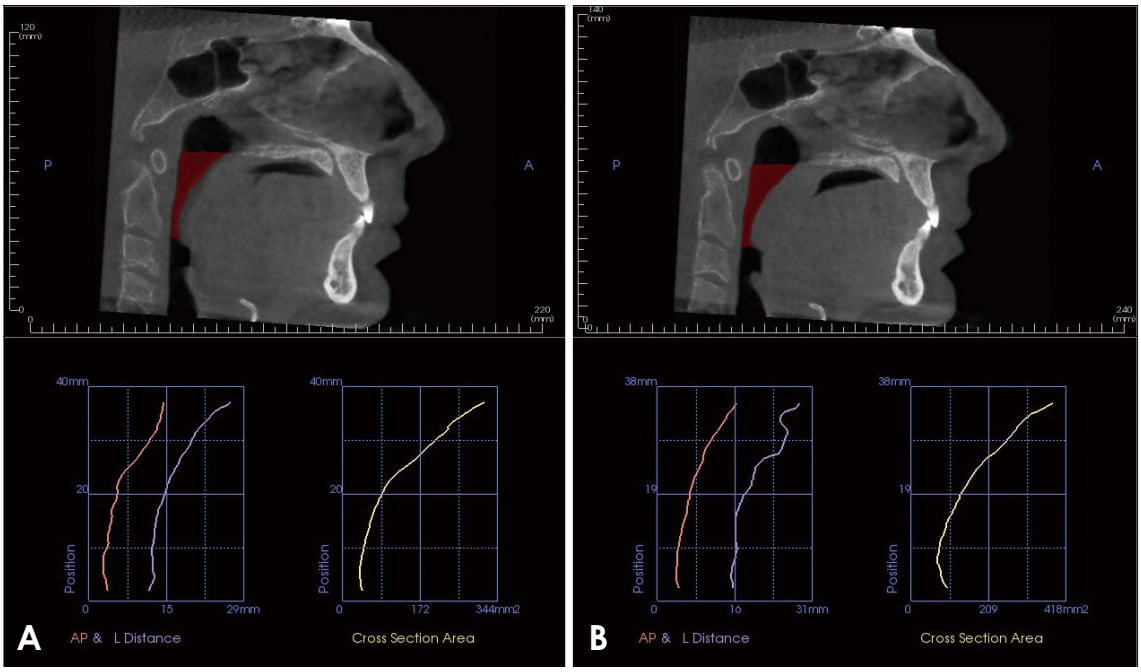

Fig. 1. An automated graph of a single obstructive sleep apnea patient along the predetermined oropharyngeal airway space shows the difference between the cross-sectional area (mm^2) and the antero-posterior and lateral dimensions (mm), using Invivo 5 software (Anatomage, San Jose, CA, USA), at the end of inspiration (A) and the end of expiration (B).

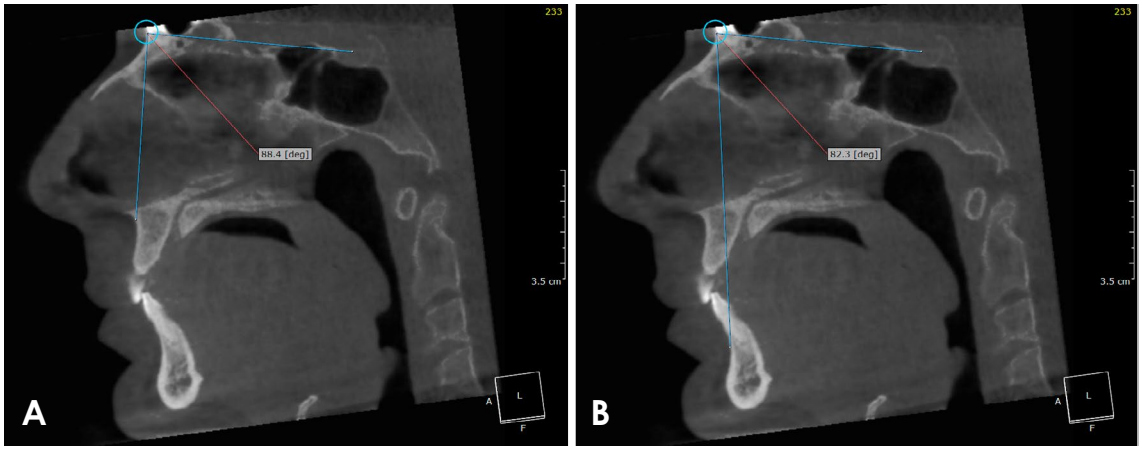

Fig. 2. SNA (A) and SNB (B) angles of a single obstructive sleep apnea patient, measured on the cone-beam computed tomography midsagittal plane using OnDemand 3D App software (Cybermed Inc, Seoul, Korea).

sequently, they were instructed to replicate these actions during the scanning process to minimize motion artifacts. The raw CBCT DICOM data were reviewed in all orthogonal planes to identify and exclude any artifacts.[22,23]

The OnDemand 3D App (Cybermed Inc, Seoul, Korea) and Invivo5 software (Anatomage, San Jose, CA, USA) were utilized to evaluate linear and volumetric measurements at the onset of both inspiration and expiration. Maximum, minimum, and average values were recorded for the cross-sectional area, anteroposterior, and lateral dimensions from both scans (Fig. 1). On the midsagittal image, the SNA (the angle formed by 2 lines: one drawn from the center of the sella turcica to the nasion, and the other from the nasion to the A point, which is the deepest part of the maxillary bone) and the SNB (the angle formed by 2 lines: one drawn from the center of the sella turcica to the nasion, and the other from the nasion to the B point, which is the deepest part of the mandibular bone) were measured (Fig. 2).[24,25] The 3D oropharyngeal airway volume and length were quantified from the posterior nasal spine (PNS) to the

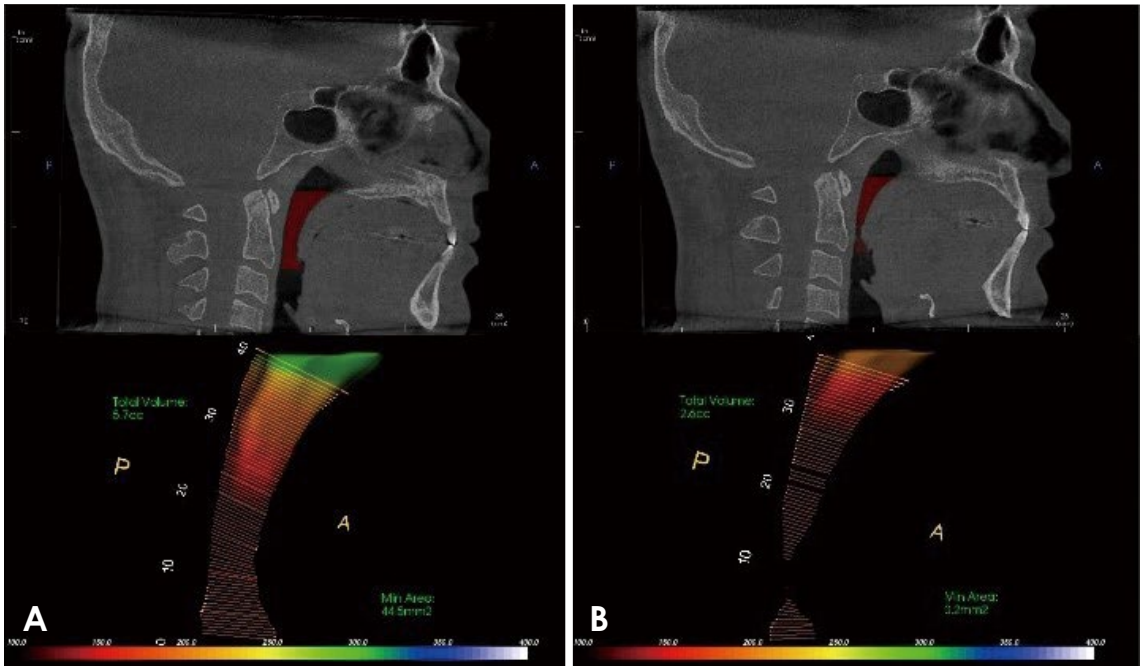

Fig. 3. An automated 2-dimensional graph of an obstructive sleep apnea patient showing the difference between the total volume of the predetermined oropharyngeal airway space (mm^3) using Invivo 5 software (Anatomage, San Jose, CA, USA) at the end of inspiration (A) and the end of expiration (B).

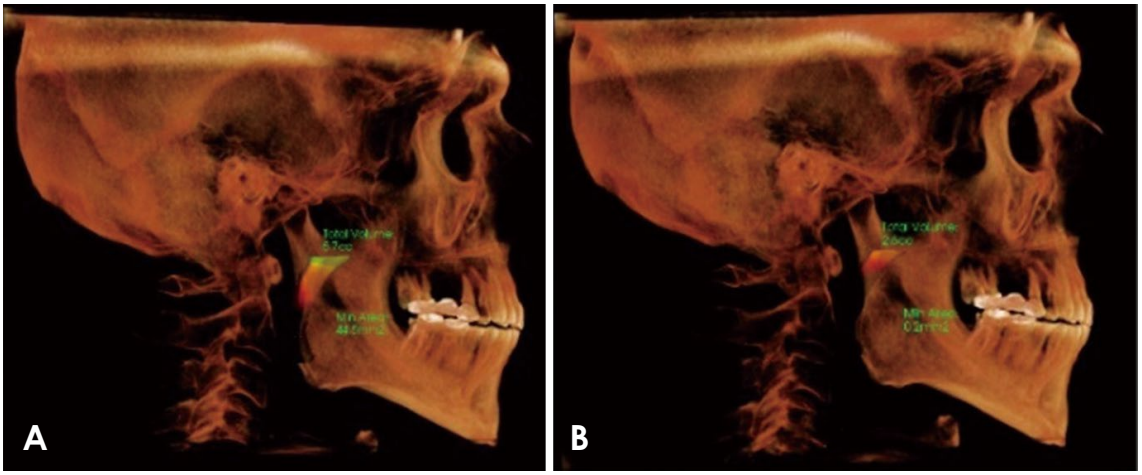

Fig. 4. An automated 3-dimensional graph of an obstructive sleep apnea patient showing the difference between the total volume of the predetermined oropharyngeal airway space (mm^3) using Invivo 5 software (Anatomage, San Jose, CA, USA) at the end of inspiration (A), and the end of expiration (B).

most anterior inferior point of the second cervical vertebra (C2), using automated 2D and 3D graphs (Fig. 3 and 4). Although the 3D rendering of the airway volume was primarily performed through automatic segmentation, some scans required semi-automatic modification. This was done by manually trimming the borders on the 3D images to correct for any excess air thresholding within the predetermined oropharyngeal airway volume.

On axial CBCT images, the pharyngeal airway morphology was classified as wide, long, or square based on the narrowest cross-sectional area (Fig. 5).[26,27] The retropalatal airway morphology was assessed from sagittal CBCT images at the mid-sagittal plane and was classified as either funnel-like, where the distance from the hard palate to the

posterior pharyngeal wall is more patent, or tunnel-like, where a vertically shaped palate with a narrower cross-section area at the level of the hard palate extends inferiorly to the velum (Fig. 6).[28]

Four oral and maxillofacial radiologists, each with varying years of experience, independently analyzed the CBCT images without exchanging any patient or clinical information or interpretations. The radiologists independently assessed the morphology of both the pharyngeal and retropalatal airways in the CBCT scans. Each radiologist conducted the linear and volumetric measurements twice, with at least a 1-month interval between evaluations.

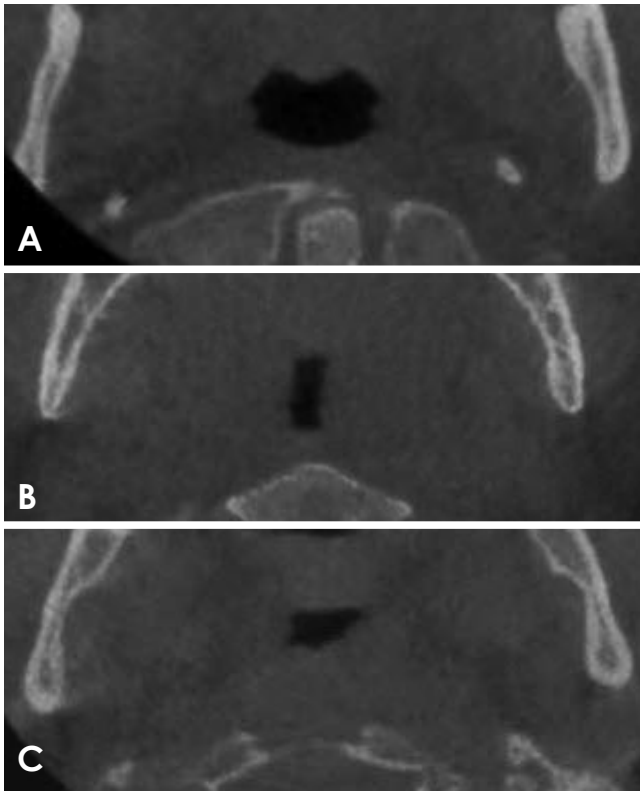

Fig. 5. Cone-beam computed tomography axial cuts at the narrowest cross-sectional area generated by the OnDemand 3D App (Cybermed Inc, Seoul, Korea), show the different pharyngeal airway morphologies at the end of inspiration. A. Wide, B. Long, C. Square.

The aim of this study was to investigate the potential correlation, whether positive or negative, between OSA severity (as measured by AHI and ESS values) and linear, volumetric, and morphological CBCT data taken at the end of both inspiration and expiration.

Data were analyzed using SPSS version 22 (IBM Corp., Armonk, NY, USA). Categorical data were presented as numbers and percentages. Continuous data were initially tested for normality using the Kolmogorov-Smirnov test. Normally distributed data were described using the mean and standard deviation, while non-normally distributed data were presented as the median and range. Statistical significance was set at a *P*-value of less than 0.05. The appropriate statistical test was then applied based on the type of data, as follows: the chi-square test for categorical variables, 1-way analysis of variance for continuous variables, and Pearson and Spearman correlations to assess relationships between continuous variables.

Results

Forty patients were initially planned to participate in this study; however, five had to drop out due to motion artifacts or overflow in the 3D rendering that could not be trimmed semi-automatically in their CBCT scans, reducing the sample size to thirty-five participants. The descriptive statistics reflect measurements at the end of inspiration and expiration, as shown in Table 1.

As indicated in Table 1, the Spearman correlation coefficient between the AHI and linear measurements at the end of inspiration showed no significant difference; likewise, no significant differences were found in the oropharyngeal measurements. The association between the AHI and linear measurements at the end of expiration, in contrast, revealed a significant difference ($P<0.05$) in the SNB angle, minimum and average cross-sectional area, and minimum lateral dimensions. The oropharyngeal

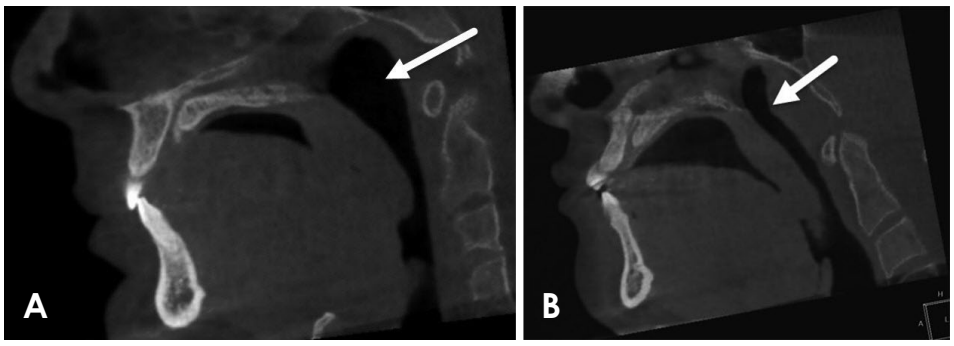

Fig. 6. Cone-beam computed tomography midsagittal cuts at the end of expiration generated by the OnDemand 3D App (Cybermed Inc, Seoul, Korea), showing funnel-like (A) and tunnel-like (B) retropalatal airway morphology.

Table 1. Correlation between the apnea-hypopnea index (AHI) and linear and oropharyngeal measurements

Linear and oropharyngeal measurements	End of inspiration				End of expiration			
	Descriptive statistics		AHI		Descriptive statistics		AHI	
	Mean ± SD	Median (range)	r	*P*-value	Mean ± SD	Median (range)	r	*P*-value
SNA	83.86 ± 4.66	84.4 (70.4-91.7)	0.193	0.274	84.17 ± 4.99	84.8 (70.1-91.7)	0.164	0.361
SNB	80.06 ± 4.16	80.5 (70.6-86.2)	0.287	0.100	80.41 ± 4.55	80.5 (70.6-86.9)	0.391	< 0.05
Maximum cross-sectional area (mm^2)	268.52 ± 103.72	252.18 (80.85-477.31)	0.180	0.300	254.0 ± 104.35	246.37 (80.85-477.31)	−0.003	0.986
Minimum cross-sectional area (mm^2)	49.93 ± 60.28	40.15 (0.12-260.58)	−0.274	0.111	46.12 ± 58.73	34.35 (0.12-258.88)	−0.410	< 0.05
Average cross-sectional area (mm^2)	119.59 ± 65.62	100.85 (32.51-320.26)	−0.024	0.890	112.24 ± 66.23	99.74 (32.51-328)	−0.352	< 0.05
Maximum antero-posterior dimensions (mm)	13.61 ± 4.18	13.96 (7.54-26.69)	−0.068	0.697	13.25 ± 4.52	13.20 (5.68-26.69)	−0.021	0.909
Minimum antero-posterior dimensions (mm)	3.19 ± 2.63	3.07 (0-11.13)	−0.095	0.586	3.0 ± 2.58	2.65 (0-10.76)	−0.263	0.139
Average antero-posterior dimensions (mm)	6.95 ± 2.17	6.85 (4.02-13.25)	0.029	0.868	6.64 ± 2.18	6.63 (3.26-12.6)	−0.135	0.452
Maximum lateral dimensions (mm)	24.64 ± 4.51	25.77 (14.77-33.19)	0.274	0.111	23.97 ± 4.76	23.14 (14.77-33.19)	0.034	0.850
Minimum lateral dimensions (mm)	9.56 ± 6.74	10.79 (0-25.01)	−0.322	0.059	8.69 ± 6.67	10.29 (0-24.5)	−0.383	< 0.05
Average lateral dimensions (mm)	15.59 ± 4.97	14.82 (8.22-29)	−0.093	0.595	15.08 ± 4.74	14.23 (8.22-27.35)	−0.331	0.06
Airway length	47.83 ± 10.78	47.0 (26.59-71.24)	0.228	0.189	47.22 ± 11.01	45.19 (26.59-71.24)	0.257	0.148
Volumetric dimensions (cc)	5.82 ± 2.84	4.8 (0.9-12.5)	0.015	0.933	5.52 ± 2.90	4.4 (0.9-12.5)	−0.229	0.200

SD: standard deviation, r: Spearman correlation coefficient

measurements showed no significant associations with the AHI in the measurements taken at the end of inspiration (Table 1).

This study investigated correlations between all the variables and the ESS score, and it was found that the airway length exhibited significant associations at the end of both inspiration and expiration. Additionally, statistically significant associations ($P<0.05$) were found between many measurements, including the SNB angle, minimum cross-sectional area, and minimum lateral dimensions, and the ESS value at the end of expiration only (Table 2).

To ensure the reliability of the data, intra-observer agreement for linear and oropharyngeal measurements was assessed at the end of both inspiration and expiration. The interclass correlation for intra-observer agreement indicated excellent consistency across all recorded data (>0.8), particularly for the oropharyngeal measurements at the end of both respiratory phases and the linear measurements at the end of expiration. However, the SNA and SNB angles exhibited good agreement (>0.70) only at the end of inspiration. Additionally, the intra-observer agreement showed a high level of concordance for all recorded data (greater than 0.8) during both the inspiratory and expiratory phases.

There was a statistically significant association ($P<0.05$) between airway morphology and the AHI at the end of inspiration only (Table 3). However, no statistically significant relationship was identified between the retropalatal airway morphology and the AHI or ESS values. A statistically significant difference ($P<0.05$) was observed in the airway morphology upon comparing the end of inspiration and expiration; however, there was no statistically significant difference in the retropalatal airway morphology (Table 4).

For the airway morphology, the 4 observers had good inter-observer kappa agreement, particularly at the end of expiration views, which exhibited excellent agreement and a high percentage of agreement (>85%). The inter-observer agreement for the retropalatal airway morphology dis-

Table 2. Correlations of linear and oropharyngeal measurements with the Epworth Sleepiness Scale (ESS)

Linear and oropharyngeal measurements	End of inspiration				End of expiration			
	Descriptive statistics		ESS		Descriptive statistics		ESS	
	Mean ± SD	Median (range)	r	*P*-value	Mean ± SD	Median (range)	r	*P*-value
SNA	83.86 ± 4.66	84.4 (70.4-91.7)	0.122	0.492	84.17 ± 4.99	84.8 (70.1-91.7)	0.189	0.293
SNB	80.06 ± 4.16	80.5 (70.6-86.2)	0.274	0.117	80.41 ± 4.55	80.5 (70.6-86.9)	0.447	<0.05
Maximum cross-sectional area (mm^2)	268.52 ± 103.72	252.18 (80.85-477.31)	0.285	0.098	254.0 ± 104.35	246.37 (80.85-477.31)	0.145	0.422
Minimum cross-sectional area (mm^2)	49.93 ± 60.28	40.15 (0.12-260.58)	−0.228	0.187	46.12 ± 58.73	34.35 (0.12-258.88)	−0.363	<0.05
Average cross-sectional area (mm^2)	119.59 ± 65.62	100.85 (32.51-320.26)	−0.014	0.937	112.24 ± 66.23	99.74 (32.51-328)	−0.286	0.106
Maximum antero-posterior dimensions (mm)	13.61 ± 4.18	13.96 (7.54-26.69)	0.071	0.685	13.25 ± 4.52	13.20 (5.68-26.69)	0.091	0.614
Minimum antero-posterior dimensions (mm)	3.19 ± 2.63	3.07 (0-11.13)	−0.238	0.168	3.0 ± 2.58	2.65 (0-10.76)	−0.242	0.175
Average antero-posterior dimensions (mm)	6.95 ± 2.17	6.85 (4.02-13.25)	0.008	0.964	6.64 ± 2.18	6.63 (3.26-12.6)	−0.121	0.503
Maximum lateral dimensions (mm)	24.64 ± 4.51	25.77 (14.77-33.19)	0.324	0.058	23.97 ± 4.76	23.14 (14.77-33.19)	0.211	0.503
Minimum lateral dimensions (mm)	9.56 ± 6.74	10.79 (0-25.01)	−0.240	0.165	8.69 ± 6.67	10.29 (0-24.5)	−0.345	<0.05
Average lateral dimensions (mm)	15.59 ± 4.97	14.82 (8.22-29)	−0.067	0.701	15.08 ± 4.74	14.23 (8.22-27.35)	−0.227	0.204
Airway length	47.83 ± 10.78	47.0 (26.59-71.24)	0.400	<0.05	47.22 ± 11.01	45.19 (26.59-71.24)	0.402	<0.05
Volumetric dimensions (cc)	5.82 ± 2.84	4.8 (0.9-12.5)	0.165	0.344	5.52 ± 2.90	4.4 (0.9-12.5)	−0.052	0.776

SD: standard deviation, r: Spearman correlation coefficient

played excellent agreement, with a high percentage (>90%) at the end of both inspiration and expiration. In addition, the intra-observer agreement for all recorded data was highly favorable (>0.8) at both the end of inspiration and expiration.

Discussion

The goal of this cross-sectional study was to investigate the relationship between CBCT radiographic and clinical findings in OSA patients, which in turn may provide a novel classification of OSA severity based on CBCT findings that are associated with the AHI classification. This objective could be achieved through the use of CBCT, as it provides an accurate 3-dimensional representation of airway structures, making it the preferred method for airway analysis. The study collected both objective and subjective CBCT radiographic data and explored their correlation with the most commonly used clinical assessment methods for determining OSA severity. Given that the AHI is the gold-standard, evidence-based tool for measuring disease severity, this study focused on analyzing the correlations between various factors and the AHI.

One of the most important factors that distinguishes apnea patients from non-apnea patients is their airway linear measurements, which include the minimum, maximum, and average cross-sectional area, anteroposterior, and lateral dimensions.[29,30] This study found a direct correlation between the disease severity, as quantified by the AHI and ESS, and the minimum values of the lateral dimension and cross-sectional area values, most notably the minimum cross-sectional area at the end of expiration. These results align with the systematic review of OSA pathophysiology conducted by Eckert et al., which indicated that disruptions in one or more non-anatomical variables might cause OSA and affect its severity.[31] Therefore, it is not necessary for all the assessed variables to be associated with OSA severity.

Table 3. Correlations of airway and retropalatal airway morphology with the apnea-hypopnea index (AHI) and Epworth Sleepiness Scale (ESS)

Morphology	End of inspiration				End of expiration			
	AHI	*P*-value	ESS	*P*-value	AHI	*P*-value	ESS	*P*-value
Airway								
Square	56.48±28.31(A)		14.45±2.04(A)		51.29±23.37		13.20±3.55	
Wide	43.99±24.29(A)	*P*=0.04*	12.36±3.41(A)	*P*=0.053	56.19±31.37	*P*=0.890	14.17±2.35	*P*=0.640
Long	97.50±3.54		16.0±1.41		60.0±0.0		14.0±0.0	
Retropalatal								
Funnel	50.21±25.73	*P*=0.182	13.59±2.81	*P*=0.409	52.38±26.62		13.67±2.71	
Tunnel	63.90±32.61		14.38±2.53		58.13±34.64		14.0±2.92	
Completely obstructed	–		–		60.0±0.0	*P*=0.936	16±0.0	*P*=0.826
Cannot be detected	–		–		64.0±0.0		15±0.0	

*statistically significant, (A): significant difference between studied groups by post-hoc Tukey test

Table 4. Correlations between airway and retropalatal airway morphology at the end of inspiration and expiration

Morphology		End of inspiration		End of expiration		*P*-value
		Number	Percentage	Number	Percentage	
Airway	Square	22	62.9	25	71.4	<0.05
	Wide	11	31.4	9	25.7	
	Long	2	5.7	1	2.9	
Retropalatal	Funnel	22	62.9	23	65.7	0.167
	Tunnel	13	37.1	12	34.3	

Compared to conventional medical CT, iCAT FLX V17-Series CBCT offers a significantly lower radiation dose and could be used to evaluate the incidence and severity of OSA, with the notable limitation that patients must remain seated during the scan.[32] In contrast, CT imaging in the supine position reflects the patient's posture during sleep, which may be more relevant for evaluating airway obstruction. Gurgel et al. conducted a systematic review and meta-analysis using various CBCT machines to acquire images in both supine and upright positions. They found that neither the volume nor the anteroposterior linear dimensions differed significantly between the two positions.[6] Consequently, even though patients were scanned in the supine position while awake (i.e., without simulating sleep) the supine position may not necessarily provide the most accurate representation.

Although CBCT exposes patients to radiation, unlike polysomnography, a rapid scan protocol was employed for each patient, completing the scan in just two seconds. Furthermore, exposure settings were carefully adjusted, and the voxel size was reduced to 0.3 mm. By also limiting the FOV to the pharyngeal airway space, the relative radiation dose was significantly minimized.

Parallel to the results of this study, which showed that end-of-expiration views differed from end-of-inspiration views, Woodson observed that during expiration, segments interact in such a way that the retroglossal level is more frequently obstructed, leading to a greater retropalatal collapse during obstructed breaths compared to non-obstructed breaths. Woodson contended that blockages during expiration often occur at the retropalatal structures, suggesting that inspiratory blockage may not be the sole indicator of an upper airway abnormality in patients.[33] Therefore, based on this assertion, all participants were imaged twice, at the end of both inspiration and expiration. Despite OSA being traditionally considered an inspiratory disease, our study highlighted that obstruction levels can also be significant at the end of expiration. This was underscored by the statistical significance of the measurements taken from the end-of-expiration views, as opposed to those from the end-of-inspiration.

Cephalometric measurements, such as SNA and SNB,

have long been documented due to an established scientific hypothesis. This hypothesis suggests that the backward displacement of the jaw compresses the muscles surrounding the pharyngeal airway, potentially leading to OSA. While these measurements are quite helpful in distinguishing OSA patients from healthy individuals, they have limited utility in assessing the severity of the condition.[27] However, in the current study, the position of the mandible was found to have a statistically significant correlation with SNB angles and predictors of severity. This implies that a retracted mandibular position, coupled with increased vertical tongue volume, may place patients at a higher risk for OSA.

Although this finding was observed exclusively at the end of expiration, it should be regarded as a statistical anomaly. To clarify, the SNB angle can be detected during both inspiration and expiration, as it demonstrates consistency across both phases. However, research by Damstra et al.[34] has assessed the reliability and measurement error associated with cephalometric analyses. These studies have shown that the measurement error can exceed 3.50 mm with a 95% confidence interval. Interestingly, the margin of error for these measurements surpassed 4°. Therefore, this may account for the observation that the SNB angle showed a statistically significant association solely at the end of expiration, despite its clinical relevance in both phases.

The human pharynx resembles a soft tube where a balance is required between the negative pressure that predisposes the airway to collapse and the contractility of the pharyngeal dilator muscle, which helps maintain patency. Furthermore, Jaffray and Siewerdsen[14] showed that the flat panel detectors used in CBCT imaging provide exceptional spatial resolution, enabling precise delineation of soft-tissue borders. This represents a key advantage of CBCT imaging: its ability to offer high contrast between different structures and to accurately determine air volume within this complex anatomy by isolating the air through thresholding. In line with the findings of Rodrigues et al., the present study found no statistically significant correlation between airway volume and the severity of OSA. This could be explained by the fact that volume measurements are taken at the peak of both inspiration and expiration, which can vary with respiratory function. Additionally, factors such as impaired upper airway muscle function during sleep, unstable respiratory control, and a low respiratory arousal threshold contribute to the pathogenesis of the disease. In other words, a reduced airway volume might be compensated for by increased muscle tonicity.[35]

Iwasaki et al. claimed that the pharyngeal airway space can be categorized into three groups in CBCT analysis, distinguished by variations in size and volume. These groups are characterized by three distinct axial shapes: wide, long, and square. The size and volume of the airway decrease progressively from the wide to the long and finally to the square shape.[26] The findings of this study suggest a strong correlation between airway morphology–specifically, the wide and square shapes–and AHI values at the end of inspiration. Due to the limited number of patients with a long airway shape, high AHI values are more commonly associated with the square shape rather than the wide. Furthermore, the statistically significant morphological differences between the end of inspiration and expiration imply that pharyngeal airway characteristics can be inferred under varying conditions.

In a "funnel-like" retropalatal airway morphology, the distance between the hard palate and the posterior pharyngeal wall is more pronounced, with the palate vertically oriented in the midsagittal plane. This orientation is parallel to the posterior pharyngeal wall and perpendicular to the hard palate. Conversely, when the palate is tilted to one side, the retropalatal airway is described as "tunnel-like." This configuration features a narrowed cross-sectional area at the level of the hard palate, which extends distally downward to the velum.[28] This study found no significant difference in the retropalatal architecture between a tunnel and a funnel at the end of both inspiration and expiration. The limited number of patients available for analysis accounts for the scarcity of data on palatal level obstruction, as underscored by the non-statistically significant difference observed between the end of inspiration and expiration.

In summary, the findings of this cross-sectional study suggest that the minimum value of the cross-sectional area, which can be automatically calculated by airway analysis CBCT software, along with the SNB angle, are both significant factors in the clinical assessment of OSA severity. Consequently, this could lead to a new classification system for OSA severity that correlates with the established AHI classification, using CBCT radiographic data. When used in conjunction with polysomnography, CBCT radiographic evaluation holds potential as a valuable diagnostic tool for the early and incidental detection of OSA.

To achieve better outcomes, it would be beneficial to plan and conduct further studies with larger sample sizes. Such studies would enable the evaluation of individuals with different AHI values, leading to more precise outcomes related to CBCT. There is also a need for additional research to determine the clinical significance of end-expi-

ration CBCT views before they can be established as a new standard for classifying disease severity. Given its potential to become a significant diagnostic tool in the near future, this technique warrants closer attention. Moreover, the medical community should increase its awareness of the importance of identifying sleep apnea. It is expected that upcoming multicenter studies will investigate the trends and advancements in the specialized application of CBCT across a broader patient population.

Conflicts of Interest: None

References

1. Benjafield AV, Ayas NT, Eastwood PR, Heinzer R, Ip MSM, Morrell MJ, et al. Estimation of the global prevalence and burden of obstructive sleep apnoea: a literature-based analysis. Lancet Respir Med 2019; 7: 687-98.
2. Peppard PE, Young T, Barnet JH, Palta M, Hagen EW, Hla KM. Increased prevalence of sleep-disordered breathing in adults. Am J Epidemiol 2013; 177: 1006-14.
3. Berry RB, Sriram P. Auto-adjusting positive airway pressure treatment for sleep apnea diagnosed by home sleep testing. J Clin Sleep Med 2014; 12: 1269-75.
4. Markun LC, Sampat A. Clinician-focused overview and developments in polysomnography. Curr Sleep Med Rep 2020; 6: 309-21.
5. Semelka M, Wilson J, Floyd R. Diagnosis and treatment of obstructive sleep apnea in adults. Am Fam Physician 2016; 94: 355-60.
6. Gurgel ML, Junior CC, Cevidanes LH, de Barros Silva PG, Carvalho FS, Kurita LM, et al. Methodological parameters for upper airway assessment by cone-beam computed tomography in adults with obstructive sleep apnea: a systematic review of the literature and meta-analysis. Sleep Breath 2022; 0: 1-30.
7. Kapur VK, Auckley DH, Chowdhuri S, Kuhlmann DC, Mehra R, Ramar K, et al. Clinical practice guideline for diagnostic testing for adult obstructive sleep apnea: an American Academy of Sleep Medicine clinical practice guideline. J Clin Sleep Med 2017; 13: 479-504.
8. Hirshkowitz M. Polysomnography challenges. Sleep Med Clin 2016; 11: 403-11.
9. Stewart SA, Skomro R, Reid J, Penz E, Fenton M, Gjevre J, et al. Improvement in obstructive sleep apnea diagnosis and management wait times: A retrospective analysis of a home management pathway for obstructive sleep apnea. Can Respir J 2015; 22: 167-70.
10. Nagappa M, Liao P, Wong J, Auckley D, Ramachandran SK, Memtsoudis S, et al. Validation of the STOP-Bang questionnaire as a screening tool for obstructive sleep apnea among different populations: a systematic review and meta-analysis. PloS one 2015; 10: e0143697.
11. Brennan HL, Kirby SD. Barriers of artificial intelligence implementation in the diagnosis of obstructive sleep apnea. J Otolaryngol Head Neck Surg 2022; 51: 16.
12. Miller JN, Berger AM. Screening and assessment for obstructive sleep apnea in primary care. Sleep Med Rev 2016; 29: 41-51.
13. Lavigne G, Herrero Babiloni A, Beetz G, Dal Fabbro C, Sutherland K, Huynh N, et al. Critical issues in dental and medical management of obstructive sleep apnea. J Dent Res 2020; 99: 26-35.
14. Jaffray D, Siewerdsen J. Cone-beam computed tomography with a flat-panel imager: initial performance characterization. Med Phys 2000; 27: 1311-23.
15. Brown AA, Scarfe WC, Scheetz JP, Silveira AM, Farman AG. Linear accuracy of cone beam CT derived 3D images. Angle Orthod 2009; 79: 150-7.
16. De Cort S, Innes J, Barstow T, Guz A. Cardiac output, oxygen consumption and arteriovenous oxygen difference following a sudden rise in exercise level in humans. J Physiol 1991; 441: 501-12.
17. Susarla SM, Abramson ZR, Dodson TB, Kaban LB. Cephalometric measurement of upper airway length correlates with the presence and severity of obstructive sleep apnea. J Oral Maxillofac Surg 2010; 68: 2846-55.
18. Epstein LJ, Kristo D, Strollo PJ Jr, Friedman N, Malhotra A, Patil SP, et al. Clinical guideline for the evaluation, management and long-term care of obstructive sleep apnea in adults. J Clin Sleep Med 2009; 5: 263-76.
19. Johns MW. Reliability and factor analysis of the Epworth Sleepiness Scale. Sleep 1992; 15: 376-81.
20. Sharkey KM, Orff HJ, Tosi C, Harrington D, Roye GD, Millman RP. Subjective sleepiness and daytime functioning in bariatric patients with obstructive sleep apnea. Sleep Breath 2013; 17: 267-74.
21. Maspero C, Giannini L, Galbiati G, Rosso G, Farronato G. Obstructive sleep apnea syndrome: a literature review. Minerva Stomatol 2015; 64: 97-109.
22. Eastwood PR, Barnes M, Walsh JH, Maddison KJ, Hee G, Schwartz AR, et al. Treating obstructive sleep apnea with hypoglossal nerve stimulation. Sleep 2011; 34: 1479-86.
23. Eckert DJ, Malhotra A, Wellman A, White DP. Trazodone increases the respiratory arousal threshold in patients with obstructive sleep apnea and a low arousal threshold. Sleep 2014; 37: 811-9.
24. Jordan AS, White DP, Lo YL, Wellman A, Eckert DJ, Yim-Yeh S, et al. Airway dilator muscle activity and lung volume during stable breathing in obstructive sleep apnea. Sleep 2009; 32: 361-8.
25. Younes M, Loewen AH, Ostrowski M, Laprairie J, Maturino F, Hanly PJ. Genioglossus activity available via non-arousal mechanisms vs. that required for opening the airway in obstructive apnea patients. J Appl Physiol 2011; 112: 249-58.
26. Iwasaki T, Hayasaki H, Takemoto Y, Kanomi R, Yamasaki Y. Oropharyngeal airway in children with Class III malocclusion evaluated by cone-beam computed tomography. Am J Orthod Dentofacial Orthop 2009; 136: 318.e1-9.
27. Massillamani F, Kailasam S, Prabhakaran A, Guntuku N. Upper aerodigestive space analysis in obstructive sleep apnea: an overview. J Dr NTR Univ Health Sci 2018; 7: 1-7.
28. Baz H, Abdalgalil AA, Zayed AM, Morsy NE, Elsobki A,

Amer A. The role of video-fluoroscopy in the assessment of obstructive sleep apnea patients: comparative study. Egypt J Otolaryngol 2023; 39: 89.
29. Ogawa T, Enciso R, Shintaku WH, Clark GT. Evaluation of cross-section airway configuration of obstructive sleep apnea. Oral Surg Oral Med Oral Pathol Oral Radiol Endod 2007; 103: 102-8.
30. Ogawa T, Enciso R, Memon A, Mah JK, Clark GT. Evaluation of 3D airway imaging of obstructive sleep apnea with cone-beam computed tomography. Stud Health Technol Inform 2005; 111: 365-8.
31. Eckert DJ. Phenotypic approaches to obstructive sleep apnoea - new pathways for targeted therapy. Sleep Med Rev 2018; 37: 45-59.
32. Enciso R, Nguyen M, Shigeta Y, Ogawa T, Clark GT. Comparison of cone-beam CT parameters and sleep questionnaires in sleep apnea patients and control subjects. Oral Surg Oral Med Oral Pathol Oral Radiol Endod 2010; 109: 285-93.
33. Woodson BT. Expiratory pharyngeal airway obstruction during sleep: a multiple element model. Laryngoscope 2003; 113: 1450-9.
34. Damstra J, Slater JJ, Fourie Z, Ren Y. Reliability and the smallest detectable differences of lateral cephalometric measurements. Am J Orthod Dentofacial Orthop 2010; 138: 546. e1-8.
35. Rodrigues MM, Pereira Filho VA, Gabrielli MF, Oliveira TF, Batatinha JA, Passeri LA. Volumetric evaluation of pharyngeal segments in obstructive sleep apnea patients. Braz J Otorhinolaryngol 2018; 84: 89-94.